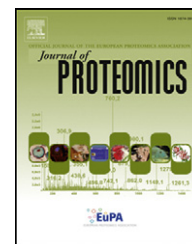


Available online at www.sciencedirect.com

ScienceDirect

www.elsevier.com/locate/jprot

Proteomic analysis of cancer and mesothelial cells reveals an increase in Mucin 5AC during ovarian cancer and peritoneal interaction



Natasha Musrap^{a,b}, George S. Karagiannis^{a,b}, Punit Saraon^{a,b}, Ihor Batruch^b, Chris Smith^c, Eleftherios P. Diamandis^{a,b,c,*}

^aDepartment of Laboratory Medicine and Pathobiology, University of Toronto, Toronto, Ontario, Canada

^bDepartment of Pathology and Laboratory Medicine, Mount Sinai Hospital, Toronto, Ontario, Canada

^cDepartment of Clinical Biochemistry, University Health Network, Toronto, Ontario, Canada

ARTICLE INFO

Article history:

Received 4 December 2013

Accepted 27 March 2014

Available online 12 April 2014

Keywords:

Ovarian cancer
Proteomics
Co-culture
Peritoneum
Metastasis
Mucin 5AC

ABSTRACT

Ovarian cancer is a highly metastatic disease that is often characterized by widespread abdominal dissemination. A hallmark of ovarian cancer progression is the attachment of malignant cells to the mesothelium and the formation of invasive peritoneal implants. Therefore, delineating factors involved in cancer-peritoneal cell interaction is critical to improving patient survival, as it may lead to the discovery of novel therapeutic targets. As such, we aimed to identify proteins that participate in this interaction by comparing the secreted proteome of a co-culture model containing ovarian cancer (OVCAR-5) and mesothelial cells (LP-9), to their respective monoculture secretomes. In total, 49 proteins were differentially secreted during cancer and mesothelial cell contact. Relative mRNA expression of candidates was performed, which revealed a significant increase in MUC5AC gene expression in cancer cells cultured in three different co-culture models (OVCAR-5 and LP-9; BG-1 and LP-9; OV-90 and LP-9). An increased expression was also observed in LP-9 cells that were co-cultured with OVCAR-5 and OV-90 cancer cells. Further immunocytochemistry analysis also confirmed increased expression of MUC5AC in ovarian cancer and peritoneal co-cultures. Overall, our analysis uncovers novel molecular markers of peritoneal metastasis, which may have potential roles in regulating the progression of the disease.

Biological significance

In this study, our objective was to focus on identifying novel mediators of ovarian cancer and peritoneal interaction using a mass spectrometry-based approach. Our analysis resulted in the discovery of both previously known and novel factors involved this interaction, and as such, these newly discovered proteins might have potential roles in cancer progression, such as invasion and adhesion. We believe that these findings add to our current knowledge and understanding of ovarian cancer progression, and will aid researchers in their future attempts in finding new targets of the disease.

© 2014 Elsevier B.V. All rights reserved.

* Corresponding author at: Mount Sinai Hospital, Joseph & Wolf Lebovic Complex, 60 Murray St., Box 32, Room L6-201, Toronto, ON M5T 3L9, Canada. Tel.: +1 416 586 8443; fax: +1 416 619 5521.

E-mail address: ediamandis@mtsinai.on.ca (E.P. Diamandis).

1. Introduction

Among gynecological malignancies, epithelial ovarian cancer (EOC) is the leading cause of death and accounts for 5% of all cancer-related deaths in North American women [1]. Given that patients are usually asymptomatic during early stages of the disease, the majority are often diagnosed at a late stage, when the survival rate is low. For the past few decades, the first-line treatment for advanced stage patients has consisted of cytoreductive surgery in combination with platinum-based chemotherapy [2]. Although these treatments elicit an initial tumor response, malignant cells eventually develop resistance, ultimately leading to cancer recurrence. Considering that overall survival rates of ovarian cancer patients have improved little since the introduction of platinum-based drugs, there is a renewed interest in the development of more effective therapeutic agents that could complement conventional approaches [3].

Ovarian cancer is often marked as a molecularly heterogeneous disease that encompasses a diverse group of tumors, which vary both histologically and genetically. As a result, treatment of the disease has proven difficult as standard chemotherapy often elicits different patient outcomes [3]. While a subset of patients present with slow growing tumors, the majority acquire rapid proliferating high-grade serous tumors, which are often characterized by late-stage presentation and intraperitoneal spread to abdominal visceral organs, which is promoted by soluble factors present within ascites fluid [3–5]. During progression of the disease, cancerous cells disseminate to the peritoneal cavity and implant on the peritoneum, which contains a thin membranous lining composed of mesothelial cells. After colonizing and breaching this layer, malignant cells are able to invade and metastasize to local organs. Since the attachment and invasion of the peritoneum are essential to the outcome of the disease, further insight into molecular processes by which this occurs will add to our current understanding about the early events of metastasis, before the cancer becomes too difficult to treat.

Numerous studies have suggested that cancer–host interactions within the tumor microenvironment are partly responsible in promoting cancer invasion and metastasis [6,7]. In particular, cancer cell interaction with the mesothelium results in the differential regulation of lipids and proteins that enhance EOC cell motility, attachment, and invasiveness [8–13]. For example, various cell adhesion and extracellular matrix components, including β 1-integrin, VCAM-1, hyaluronan, and CD44, have been shown to facilitate cancer attachment and invasion of the peritoneum [9–11,14–16]. However, the underlying mechanisms of this biological interaction still remain largely unknown, as there may be many other molecular factors that play a role. Therefore, increased knowledge of this tumor–host interface may lead to the discovery of novel therapeutic targets. In turn, abrogation of these targets may inhibit peritoneal dissemination and enhance patient survival.

In the past decade, high-throughput proteomics has been an efficient discovery tool for mining biological fluids and tissues in the search for soluble biomarkers that could be used for the early detection of various pathologies. However, recent studies have adopted this technique to identify proteins and associated pathways that become altered during various stages of disease

pathogenesis, particularly, through the use of co-culture model systems that reflect specific biological states [17–20]. In the present study, we aimed to delineate differentially secreted proteins during ovarian cancer and mesothelial cell interaction by conducting a global secretome analysis using a mass spectrometry (LC-MS/MS)-based approach. In our attempts, we utilized a direct in vitro co-culture model of an ovarian cancer cell line, OVCAR-5, and a mesothelial cell line, LP-9, and compared the secretome composition of this model to that of OVCAR-5 and LP-9 secretomes. Our proteomic analysis resulted in the overall identification of 2554 non-redundant proteins, whereby a subset was found to be differentially expressed in our co-culture model, which may reflect biological interactions at the cancer–peritoneal interface. Specifically, from our proteomic analysis, mucin 5AC (MUC5AC) was identified as our top candidate, which was also elevated in two other co-culture models (BG-1/LP-9 Co and OV-90/LP-9 Co) and in patient ascites fluid. Taken together, our approach reveals several proteins that are elevated during the interaction between ovarian cancer cells and the peritoneum. Further investigation of their role in EOC pathogenesis is warranted.

2. Materials and methods

2.1. Cell lines

The human ovarian cancer cell line, OVCAR-5, was obtained from the Fox Chase Cancer Centre (Philadelphia, PA). BG-1 cells were provided by Dr. Henri Rochefort (Montpellier, France), while the OV-90 (ATCC CRL-11732) cell line was purchased from the American Type Culture Collection (ATCC, Manassas, VA). Primary human peritoneal mesothelial cells, LP-9, were purchased from the Coriell Institute for Medical Research (Camden, NJ). All ovarian cancer cell lines were grown in RPMI 1640 medium (Wisent) supplemented with 10% characterized fetal bovine serum (FBS) (Thermo Scientific). LP-9 peritoneal cells were grown in a 1:1 mixture of Ham's F-12 medium/Medium 199 (Invitrogen) containing 10% FBS, 10 ng/mL epidermal growth factor (Reprokine Ltd.), and 0.4 μ g/mL hydrocortisone (Sigma Aldrich). All cell lines were cultured in a humidified incubator adjusted to 37 °C with an atmosphere of 5% CO₂.

2.2. Establishment of monocultures and co-cultures of cancer and peritoneal cells

2.2.1. Proteomic analysis

OVCAR-5 and LP-9 cell monocultures were established by culturing each cell line in three T175 cm² flasks using their respective growth media containing 10% FBS, as described above. Upon reaching 70% confluency, cells were washed three times with PBS (Wisent) and grown in 30 mL of chemically defined Chinese hamster ovary serum-free medium (Invitrogen) supplemented with 8 mM L-glutamine (Invitrogen) for 48 h. Co-cultures were also constructed in triplicates using T175 cm² flasks, as OVCAR-5 cells were plated over a confluent layer of LP-9 cells. Briefly, OVCAR-5 cells were washed, trypsinized, centrifuged (5 min at 450 \times g), washed with PBS, resuspended in LP-9 media containing 10% FBS, and subsequently added to the

monolayer of LP-9 cells. Cells were allowed to attach overnight before the co-cultures were washed three times with PBS and changed to serum-free media. After 48 h, conditioned media (CM) was collected from each flask and centrifuged at 450 ×g for 5 min to remove cellular debris. Total protein was measured using a Coomassie Blue (Bradford) total protein assay. Approximately 1 mg of total protein from each replicate was subjected to further LC-MS/MS sample processing as described below.

2.2.2. mRNA expression analysis

Indirect one way co-cultures were constructed by using conditioned media from OVCAR-5 cells to stimulate LP-9 cells, and vice versa. Stimulations were done for approximately 24 h, and cell pellets were collected and used for mRNA expression analysis.

Indirect two way co-cultures were also developed using cell culture inserts with pore sizes of 0.4 μm (Becton Dickinson and Company, NJ, USA). LP-9 cells were plated in six-well plates, which were then overlaid with cell culture inserts containing OVCAR-5, OV-90, or BG-1 ovarian cancer cells. After co-culturing for 24 h in normal growth media with 10% FBS, cell pellets were collected and washed, before undergoing total RNA extraction.

2.3. Sample processing for LC-MS/MS-based protein identification of secretomes

Conditioned media were dialyzed using a 3.5 kDa molecular weight cut-off porous membrane (Spectrum Laboratories, Inc., Compton, CA) in 4 L of 1 mM ammonium bicarbonate buffer at 4 °C overnight. A total of three buffer exchanges were completed before freezing samples at –80 °C. Frozen samples were lyophilized to complete dryness using a ModulyoD Freeze Dryer (Thermo Electron Corporation). Samples were then denatured with 8 M urea, reduced with 200 mM dithiothreitol at 50 °C for 30 min, and alkylated with 500 mM iodoacetamide with shaking in the dark for 1 h. Using NAP5 sephadex columns (GE Healthcare), samples were then desalted, frozen at –80 °C, and lyophilized to complete dryness. Following lyophilization, samples were resuspended in 50 mM ammonium bicarbonate, water, and methanol. The samples were digested with trypsin overnight at 37 °C using a 1:50 trypsin/total protein concentration ratio. Mobile phase buffer A (0.26 M formic acid, 10% acetonitrile; pH 2–3) was added to each digested sample, which was then subjected to strong cation exchange (SCX).

2.4. Strong cation exchange (SCX)-high performance liquid chromatography (HPLC)

Tryptic peptides were fractionated with an Agilent 1100 system using a one hour gradient of mobile phase A buffer, and peptides were eluted with the same buffer as mobile phase A SCX buffer with the addition of 1 M ammonium formate. Samples were then injected into a 500 μL loop that was connected to a PolySULFOETHYL aspartamide column containing an anionic polymer with pore sizes of 200 Å and a diameter of 5 μm (The Nest Group Inc., Southborough, MA). The fractionation was monitored at a wavelength of 280 nm, and fractions that were collected every 2 min from 24 to 50 min with a flow rate of 260 μL/min were used for further

analysis. Fractions with a low peak absorbance were pooled, which resulted in a total of 12 fractions per sample replicate. Each fraction was diluted in order to obtain a final concentration of approximately 5% acetonitrile.

2.5. Mass spectrometry (LC-MS/MS)

Peptides were purified and extracted from SCX fractions using OMIX C₁₈ Pipette Tips, and were eluted in 70% MS Buffer B (90% acetonitrile, 0.1% formic acid, 10% water, and 0.02% trifluoroacetic acid) and 30% MS Buffer A (5% acetonitrile, 0.1% formic acid, 95% water, and 0.02% trifluoroacetic acid). A total of 40 μL of each fraction was loaded onto an EASY-nLC system (Proxeon Biosystems, Odense, Denmark), which was directly transferred online to a LTQ-Orbitrap mass spectrometer (Thermo Fisher Scientific). Using a 5 cm C18 analytic column, peptides from each fraction were resolved using a 90 minute gradient of MS Buffers A and B, in data-dependent mode. Peptides were subjected to one full MS1 scan (450–1450 m/z) in the Orbitrap (resolution 60,000), and six MS2 data-dependent scans in the linear ion trap mass analyzer. Using charge state screening, only charge states of +2 and +3 were selected for MS2 fragmentation.

2.6. Database search and protein identification

RAW files containing mass spectra of identified peptides were searched and analyzed on Mascot (Matrix Science, London, UK, version 2.2.0) to create DAT and MGF files. The resulting MGF files were analyzed in X!Tandem (Global Proteome Machine Manager, version 2006.06.01) using the International Protein Index (IPI) human database (version 3.62), in which XML files were generated. The resulting XML files along with DAT files were merged using Scaffold software (Proteome Software Inc., v. 2.06), which produced a list of proteins identified in each sample. Using the X!Tandem Log E and Mascot ion-score filters within Scaffold, we adjusted for false discovery rates (FDRs) of approximately 1% at the protein level. The FDR was calculated using the following formula: $(2 \times \text{\#false positives}) / (\text{\#false positive} + \text{\#true positive}) \times 100$, where false positives were proteins that were identified by sequences in the reverse database, and true positives were proteins that were identified by sequences in the forward database. Finally, protXML files were exported from Scaffold and uploaded into ProteinCenter (Proxeon Biosystems).

2.7. Candidate filtering and pathway analysis

From the protein lists generated, proteins identified in OVCAR-5 and LP-9 monoculture datasets were excluded from those present in the co-culture secretome, using comparison tools provided in ProteinCenter. To establish more stringent criteria, proteins that were unique to OVCAR5/LP9 co-cultures were filtered for two peptide hits, in order to increase the confidence in our candidates. Since cytosolic-derived proteins are released into conditioned media as a result of cell death during cell culture, secreted/membrane proteins were enriched for, by selecting for proteins that contain a signal peptide and those that were deemed 'extracellular' or 'membrane' according to Gene Ontology (GO) cellular localization annotations using ProteinCenter. Moreover, spectral counts of each protein were

considered when selecting candidates, as proteins that had high spectral counts in the co-cultures and low counts in monocultures were also considered as potential regulators of EOC progression. Generally, the remaining candidates were chosen if their spectral count in co-culture condition was at least two fold greater than the average spectral count in both monocultures. ProteinCenter was also used to categorize proteins according to their molecular and biological functions using assigned GO annotations. Protein networks of putative candidates were generated using Ingenuity Pathway Analysis software (Ingenuity® Systems, www.ingenuity.com), which provided the top network functions of secreted proteins that displayed differential secretion during cancer-peritoneal interaction.

2.8. Cell migration assay

To determine the effect of cancer cell migration in response to treatment with LP-9 conditioned media, cell scratch assays were constructed by seeding OVCAR-5 cells in 6-well plates. Upon reaching confluency, a scratch across the middle of each well was made using a pipette tip. Cells were then washed three times with PBS to remove cellular debris, and treated with either serum-free media or LP-9-derived conditioned medium for a period of 48 h. Changes in cell migration were assessed by examining the ability of cancer cells to elicit wound repair, which was measured by calculating the mean wound length over time.

2.9. RNA extraction, cDNA synthesis, and quantitative polymerase chain reaction (qPCR)

Purification of total RNA was performed using the RNeasy kit (Qiagen). The samples used for RNA extraction were as follows: OVCAR-5 cells stimulated with conditioned media from LP-9 cells, OVCAR-5 cells in serum-free conditions, LP-9 cells in serum-free conditions, and LP-9 cells stimulated with conditioned media from OVCAR-5 cells. cDNA was generated using a SuperScript First-Strand cDNA synthesis kit (Invitrogen), and subsequently used for qPCR to evaluate relative gene expression. TATA-binding protein (TBP) was used as a housekeeping gene to measure relative expression, as its expression was not expected to vary across the different experimental conditions. Gene expression analysis was performed on the following genes: PSCA, MUC4, CD109, LOXL4, LTBP1, PPP3CA, ITGB4, INHBA, HYAL1, COL6A3, LRG1, CAP1, PTPRK, CST6, MUC5AC, TFPI2, CXCL5, PLEC1, and GDF15 (forward and reverse primer sequences are listed in Supplementary Table 1). mRNA expression analysis was also performed on OVCAR-5, OV-90, BG-1, and LP-9 cells grown as indirect two-way co-cultures using transwell inserts with 0.4 μm pore sizes (Becton Dickinson). Quantitative PCR was performed using 1X SYBR Green PCR Master Mix (Applied Biosystems) and levels of mRNA transcripts were measured on a 7500 ABI system. Fold changes of gene expression between stimulated and control conditions were displayed as a heat map using FiRe version 2.2 [21].

2.10. MUC5AC enzyme-linked immunosorbent assay (ELISA) analysis in EOC ascites and benign cyst fluids

All biological fluids were obtained with informed consent and Institutional Review Board approval, which include ovarian

cancer ascites fluid from advanced stage ovarian cancer patients ($n = 8$) and serous ovarian cyst fluid ($n = 10$) from benign neoplasms. Levels of MUC5AC were measured using an enzyme-linked immunosorbent assay kit according to the manufacturer's instructions (Usn Life Science Inc.).

2.11. Immunocytochemistry

LP-9, OVCAR-5, OV-90, and BG-1 cells were plated in 12-well plates in regular growth medium. Co-cultures of LP-9/OVCAR-5, LP-9/OV-90, and LP-9/BG-1 cells were constructed as described above. After reaching 80% confluency, all cell cultures were washed three times with PBS and grown in serum-free media for 2 days. Cells were then washed twice with PBS, and fixed with 4% paraformaldehyde for 15 min at room temperature. Following fixation, cells were washed three times with ice-cold PBS and permeabilized with 0.2% Tween-20 for 10 min. After three 5-minute washes with PBS, cells were then treated with 1% BSA in PBST for a period of 30 min. Afterwards, cells were incubated with MUC5AC primary antibody (1:500, Abcam) in 1% BSA in PBST at 4 °C overnight. The following day, all cells were rinsed three times for 5 min with PBS, and endogenous peroxidase was blocked with 3% H_2O_2 for 20 min. After washing, cells were incubated with horseradish peroxidase-conjugated secondary antibody in 1% BSA (1:1000) for 1 h. Finally, cells were then rinsed three times with PBS, and incubated with DAB chromogenic substrate for approximately 10 min or until color developed. Cells were then washed and stored in PBS. No antibody controls for all monocultures and co-cultures were also performed, as well as an IgG1 isotype control for OVCAR-5/LP-9 co-cultures. Staining was visualized using a light microscope, and images were captured using the OLYMPUS Q-Color3 imaging system.

3. Statistical analysis

All statistical significance tests on scratch assay and gene expression data were analyzed using independent t-tests (Minitab, v. 14). MUC5AC levels measured in ovarian cancer ascites and benign cyst fluids were compared using the Mann-Whitney U test (GraphPad Prism, v.6.03). Results comparing different conditions were considered significant if the p-value was less than or equal to 0.05. The Fisher exact test was calculated using SPSS Statistical Software.

4. Results

4.1. LP-9 conditioned media promote in vitro cancer cell migration

The progression of ovarian cancer is marked by enhanced cancer motility, as malignant cells adopt a migratory behavior and travel through the extracellular matrix to distant metastatic sites. However, in this study, we were only interested in performing a global characterization of protein alterations that occur between cancer and peritoneal cells. Alternatively, cancer cells can remain in ascites fluid and form multicellular aggregates, which preferentially attach to the peritoneum.

Previous studies have established that media conditioned by mesothelial cells can increase the migratory potential of ovarian cancer cells, partially through the secretion of fibronectin as well as other unknown soluble factors [13]. Therefore, to assess whether this observation could be recapitulated with our cell lines, we constructed preliminary in vitro scratch assays by using LP-9 medium conditioned by LP-9 cells for 48 h to stimulate confluent monolayers of OVCAR-5 cells that had been scratched with a pipette tip, creating a wound between the cells (Fig. 1A). After 24 and 48 h post-stimulation, there was significant increase in wound closure by treated cancer cells, compared to non-stimulated cells, which was evaluated by calculating the mean wound length (p < 0.05) (Fig. 1A). As such, these observations support previous findings that suggest that soluble factors from mesothelial cells can either induce cancer cell migration, or stimulate cancer cells to secrete factors that lead to enhanced cell motility.

4.2. Proteomic profiling of monoculture and co-culture CM

We sought to identify proteins that displayed elevated secretion during cancer–mesothelial interaction, which could provide biological insight into the mechanisms that modulate peritoneal metastasis. Therefore, we conducted a comparative proteomic analysis of the secretome, in which we compared the secretion of proteins identified in conditioned media of a mesothelial cell

line (LP-9) and an ovarian cancer cell line (OVCAR-5), to those present in CM of LP-9/OVCAR-5 direct co-cultures using an experimental outline as shown in Fig. 1B. Overall, our analysis resulted in the identification of 1435 proteins secreted by LP-9 cells, 1646 by OVCAR-5 cells, and 1586 by LP-9/OVCAR-5 co-cultures with a minimum of one peptide (Fig. 1C and Supplementary Tables A.2–A.4). Integrating all three datasets revealed a total of 2554 non-redundant proteins, of which 189 proteins were specific to the co-cultures, as they were not detected in the CM of either monoculture (Fig. 1D). Moreover, in addition to identifying candidate proteins that were exclusively present in the co-culture dataset, a subset of proteins displayed lower secretion in monoculture secretomes compared to co-cultures based on spectral counting.

To limit our dataset of proteins to a smaller subset of candidates involved in cancer–peritoneal interaction, we applied several filtering criteria that would eliminate proteins that were not secreted or were likely to be false hits. Firstly, using the 189 proteins that were unique to the co-culture secretome, we filtered for proteins that were identified with a minimum of two peptides using tools provided in ProteinCenter, which narrowed down our initial list to 50 proteins (Fig. 2A). Moreover, as it is well recognized that uncontrolled cell death occurs during regular cell culture growth conditions, the secretome contains several proteins that are typically deemed cytosolic. Thus, to remove these intracellular contaminant proteins, the remaining proteins were categorized based on their cellular localization using Gene

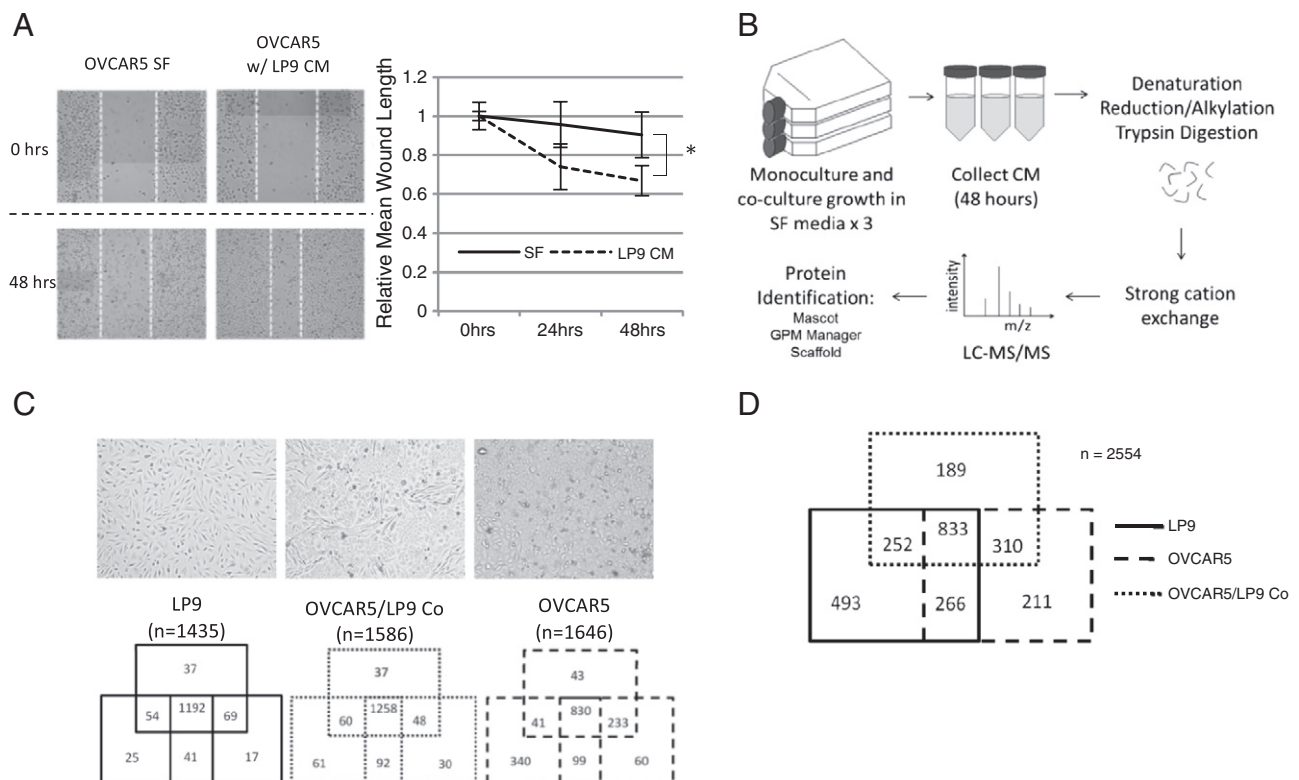


Fig. 1 – Cell scratch assay and identification of proteins present in LP-9, OVCAR-5, and LP-9/OVCAR-5 co-culture conditioned media. **A)** Cell scratch assay of OVCAR-5 cells treated with conditioned media from LP-9 cells and relative mean wound length at 0 h, 24 h, and 48 h post-treatment with LP-9 CM (*, p < 0.05, independent t-test). **B)** Experimental workflow used for protein identification. **C)** Total number of proteins identified with ≥ 1 peptides in the three replicates of each condition. **D)** Combining all identified proteins revealed 189 proteins unique to cancer–mesothelial co-cultures (minimum 1 peptide).

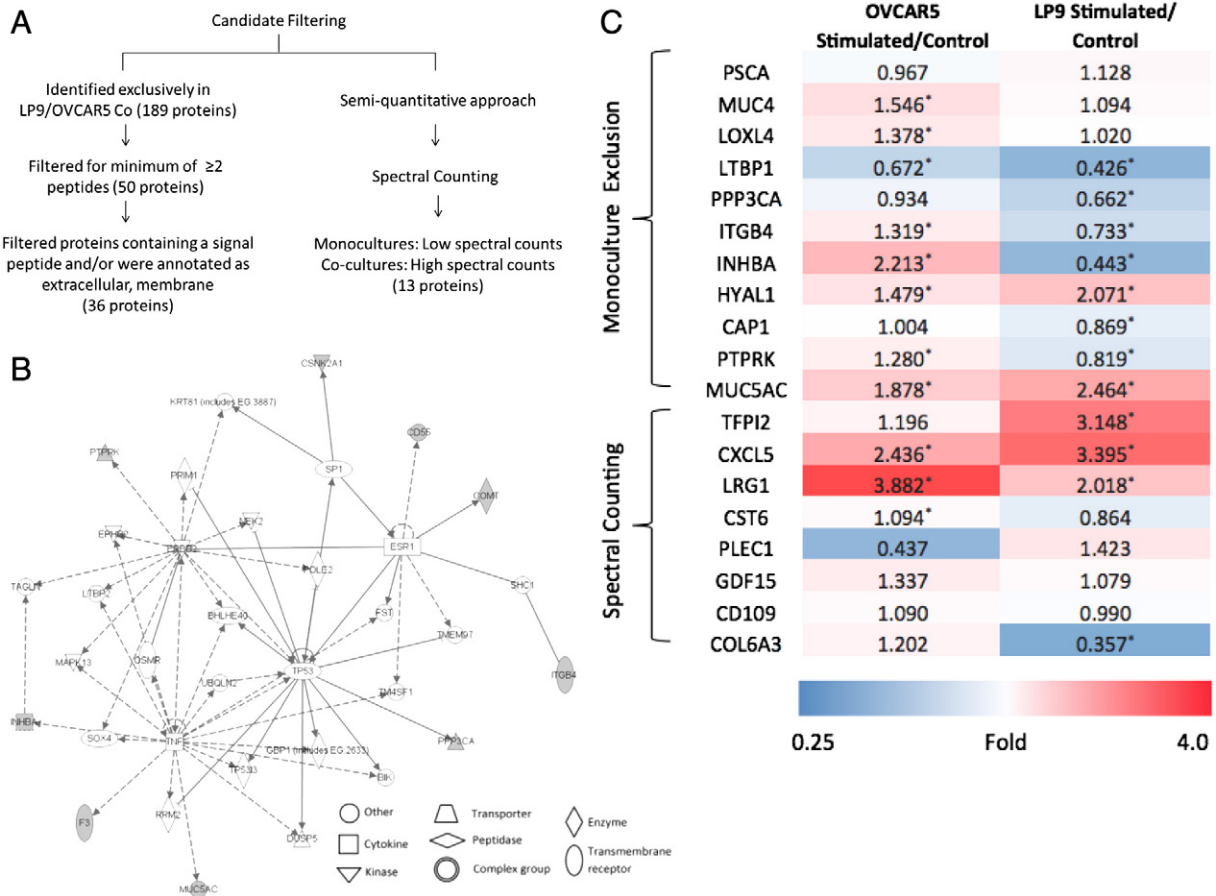


Fig. 2 – Filtering, IPA analysis, and mRNA expression of selected candidates. A) Filtering candidates using two approaches: exclusion and spectral counting. B) Ingenuity Pathway Analysis clustered candidate proteins in networks belonging to molecular transport, cancer, cell-to-cell signaling and interaction, and cell death and survival. Gene and proteins are depicted as nodes (shaded/gray nodes represent upregulated proteins in our co-culture model; white nodes depict genes/proteins that were incorporated by Ingenuity Knowledge Base to build genes/proteins into networks). Nodes connected by solid lines indicate a direct relationship, whereas dotted lines depict an indirect relationship. C) mRNA expression of selected genes displayed as a heatmap. Ratios represent fold changes in expression of stimulated cells over control cells. Red corresponds to increased gene expression, whereas blue illustrates reduced expression (*, P ≤ 0.05, Student’s t-test).

Ontology annotations available through Protein Center software. Specifically, proteins that were annotated as “extracellular” or “membrane” and/or contained a signal peptide were enriched for, which generated a total list of 36 proteins (Table 1). As mentioned earlier, differential secretion of proteins was also assessed by using normalized spectral counts. Secreted or membrane proteins that had lower spectral counts in monocultures compared to co-cultures were also considered as possible candidates, which resulted in 13 additional proteins that are summarized in Table 2. Overall, a total of 49 candidate proteins showed elevated secretion during cancer–peritoneal interaction. Further Gene Ontology classification revealed that the top biological processes included response to stimuli and metabolic processes, whereas top molecular functions of candidate proteins included catalytic activity and protein binding (Supplementary Fig. 1A and B).

After delineating our list of candidate proteins, Ingenuity Pathway Analysis was used to uncover biological networks related to our candidates, as well as pinpoint potential

protein–protein interactions. In summary, the top-associated network functions included molecular transport, protein trafficking, lipid metabolism, cancer, cell-to-cell signaling and interactions, and cell death and survival. Interestingly, candidates were linked to common pathways including TP53, TNF, and ESR1 (Fig. 2B), which have all been implicated in ovarian cancer pathogenesis [22–24].

4.3. Gene expression analysis of top candidates in OVCAR-5/LP-9 indirect one-way co-cultures

To determine whether the gene expression of our candidates correlates with our proteomic results, we performed real-time PCR on a subset of candidate proteins (PSCA, MUC4, CD109, LOXL4, LTBP1, PPP3CA, ITGB4, INHBA, HYAL1, COL6A3, LRG1, CAP1, PTPRK, CST6, MUC5AC, TFPI2, CXCL5, PLEC1, and GDF15) on indirect co-cultures of LP-9 and OVCAR-5 cells. Briefly, conditioned media was collected from OVCAR-5 cells and was used to stimulate LP-9 cells, and vice versa. The

Table 1 – Secreted proteins identified exclusively in LP9/OVCAR5 co-culture supernatants (≥ 2 peptides). Each protein was present in at least two of the three replicates.

| Accession | Gene symbol | Protein description | No. unique peptides | Mean spectral count \pm SD | # Replicates with detectable protein |
|-------------|-------------|--|---------------------|------------------------------|--------------------------------------|
| IPI00216393 | CLTA | Isoform non-brain of clathrin light chain A | 4 | 2.3 \pm 1.5 | 3 |
| IPI00411680 | PCMT1 | Isoform 1 of protein-L-isoaspartate(D-aspartate) O-methyltransferase | 2 | 1.7 \pm 0.6 | 3 |
| IPI00639931 | CAP1 | Isoform 2 of adenylyl cyclase-associated protein 1 | 10 | 9.0 \pm 1.0 | 3 |
| IPI00216550 | CD55 | Isoform 1 of complement decay-accelerating factor | 3 | 1.7 \pm 0.6 | 3 |
| IPI00306402 | LOXL4 | Lysyl oxidase homolog 4 | 3 | 1.7 \pm 1.2 | 3 |
| IPI00550451 | PPP1CA | Serine/threonine-protein phosphatase PP1-alpha catalytic subunit | 7 | 10.7 \pm 4.0 | 3 |
| IPI00643525 | C4A | Uncharacterized protein | 23 | 29.3 \pm 4.7 | 3 |
| IPI00303207 | ABCE1 | ATP-binding cassette sub-family E member 1 | 2 | 1.7 \pm 0.6 | 3 |
| IPI00154451 | MMS19 | cDNA FLJ55586, highly similar to MMS19-like protein | 3 | 3.0 \pm 1.7 | 3 |
| IPI00168847 | HYAL1 | Isoform 2 of hyaluronidase-1 | 4 | 5.0 \pm 1.0 | 3 |
| IPI00027422 | ITGB4 | Isoform beta-4C of Integrin beta-4 | 5 | 3.7 \pm 1.2 | 3 |
| IPI00015756 | PTPRK | Isoform 1 of Receptor-type tyrosine-protein phosphatase kappa | 5 | 6.3 \pm 4.0 | 3 |
| IPI00791006 | MUC4 | Mucin-4 isoform a | 7 | 4.7 \pm 3.1 | 3 |
| IPI00028670 | INHBA | Inhibin beta A chain | 5 | 3.3 \pm 1.2 | 3 |
| IPI00045536 | CHID1 | Isoform 3 of chitinase domain-containing protein 1 | 3 | 1.0 \pm 1.0 | 2 |
| IPI00019038 | LYZ | Lysozyme C | 2 | 4.3 \pm 0.6 | 3 |
| IPI00218830 | NMT1 | Isoform short of glycolipid N-tetradecanoyltransferase 1 | 2 | 1.7 \pm 1.2 | 3 |
| IPI00883772 | GAA | Lysosomal alpha-glucosidase preproprotein | 12 | 12.3 \pm 2.5 | 3 |
| IPI00514894 | KPNA6 | Karyopherin alpha 6 | 2 | 2.0 \pm 0 | 3 |
| IPI00010338 | F3 | Tissue factor | 4 | 2.3 \pm 1.5 | 3 |
| IPI00011284 | COMT | Isoform membrane-bound of catechol O-methyltransferase | 3 | 1.3 \pm 1.2 | 2 |
| IPI00029629 | TRIM25 | E3 ubiquitin/ISG15 ligase TRIM25 | 2 | 1.0 \pm 1.0 | 2 |
| IPI00217952 | GFPT1 | Isoform 1 of glucosamine—fructose-6-phosphate aminotransferase [isomerizing] 1 | 2 | 1.0 \pm 2.0 | 2 |
| IPI00000728 | USP15 | Isoform 1 of ubiquitin carboxyl-terminal hydrolase 15 | 3 | 1.7 \pm 1.2 | 3 |
| IPI00007321 | LYPLA1 | cDNA FLJ60607, highly similar to Acyl-protein thioesterase 1 | 2 | 1.0 \pm 0 | 3 |
| IPI00016613 | CSNK2A1 | CSNK2A1 protein | 2 | 1.3 \pm 0.6 | 3 |
| IPI00032406 | DNAJA2 | Dnaj homolog subfamily A member 2 | 2 | 1.3 \pm 0.6 | 3 |
| IPI00179415 | PPP3CA | Isoform 1 of Serine/threonine-protein phosphatase 2B catalytic subunit alpha isoform | 3 | 1.3 \pm 0.6 | 3 |
| IPI00013446 | PSCA | Prostate stem cell antigen | 3 | 8.3 \pm 0.6 | 3 |
| IPI00215899 | SRPX | Isoform 2 of Sushi repeat-containing protein SRPX | 2 | 1.7 \pm 0.6 | 3 |
| IPI00103397 | MUC5AC | Mucin-5AC (Fragment) | 20 | 29.0 \pm 6.6 | 3 |
| IPI00218676 | IL1RL1 | Isoform B of interleukin-1 receptor-like 1 | 2 | 1.0 \pm 1.0 | 2 |
| IPI00893273 | LTBP1 | Latent-transforming growth factor beta-binding protein 1 isoform 5 precursor | 16 | 9.0 \pm 4.4 | 3 |
| IPI00103480 | LIPH | Lipase member H | 2 | 1.0 \pm 1.0 | 2 |
| IPI00217778 | PLTP | Isoform 2 of phospholipid transfer protein | 3 | 12.7 \pm 1.5 | 3 |
| IPI00024650 | SLC16A1 | Monocarboxylate transporter 1 | 2 | 0.7 \pm 0.6 | 2 |

expression of the above genes in each cell type was compared to cells grown in serum-free media, which is displayed as a heat map in Fig. 2C with fold-change ratios. As expected, mRNA fold changes of some genes did not parallel with our proteomic data, which could be a result of post-translational processes such as protein degradation, half life, and shedding mechanism, or because direct cell contact between the two cell types may be required for gene activation. Of the genes analyzed, there was a significant increase in mRNA expression levels for HYAL1, LRG1, MUC5AC, TFPI2, and CXCL5 ($p < 0.05$, independent t-test).

4.4. MUC5AC gene expression is increased in OVCAR-5/LP-9, OV-90/LP-9, and BG-1/LP-9 co-cultures (QPCR)

Based on our proteomic discovery data, mucin 5AC was our most attractive candidate as it displayed the highest spectral counts in cancer-mesothelial co-culture secretomes in comparison to all other candidates that were not identified in either cancer or

mesothelial cell line conditioned media. Moreover, its gene expression was significantly elevated in indirect one-way co-cultures. Therefore, to evaluate its expression in other cell line models, gene expression analysis was performed in cells engaged in a two-way indirect co-culture, which is a more favorable system as both cell types share the same media and are able to exchange soluble factors. Specifically, OVCAR-5, OV-90, BG-1 and LP-9 cells were co-cultured together using transwell inserts of 0.4 μm pore sizes. Significant increases in MUC5AC expression were observed in OVCAR-5, OV-90, and BG-1 cells that were co-cultured with mesothelial cells, as shown in Fig. 3 ($p < 0.05$, independent t-test). Similarly, MUC5AC also displayed increased expression in LP-9 cells that were co-cultured with either OVCAR-5 or OV-90 cells ($p < 0.05$, independent t-test).

4.5. MUC5AC is elevated in EOC ascites fluid (ELISA)

Ascites fluid contains a rich milieu of secreted proteins and soluble factors that are shed by malignant cells and surrounding

Table 2 – Secreted proteins elevated in LP9/OVCAR5 co-cultures in comparison to cancer and mesothelial secretomes (based on average normalized protein spectral counts). Each protein was identified in all three co-culture replicates.

| Accession | Gene symbol | Protein description | Mean spectral count ± SD (LP9) | Mean spectral count ± SD (OVCAR5) | Mean spectral count ± SD (LP9/OVCAR5 Co) |
|-------------|-------------|---|--------------------------------|-----------------------------------|--|
| IPI00152540 | CD109 | CD109 isoform 1 of CD109 antigen | 5.3 ± 1.5 | 6.7 ± 1.5 | 35.0 ± 1.7 |
| IPI00022200 | COL6A3 | COL6A3 isoform 1 of collagen alpha-3(VI) chain | 3.3 ± 1.2 | N/A | 10.0 ± 6.9 |
| IPI00022417 | LRG1 | LRG1 leucine-rich alpha-2-glycoprotein | N/A | 4.0 ± 5.2 | 30.3 ± 2.9 |
| IPI00019954 | CST6 | CST6 cystatin-M | N/A | 1.7 ± 2.1 | 17.3 ± 3.2 |
| IPI00009198 | TFPI2 | TFPI2 tissue factor pathway inhibitor 2 | 6.3 ± 2.5 | N/A | 10.7 ± 2.1 |
| IPI00292936 | CXCL5 | CXCL5 C–X–C motif chemokine 5 | 6.0 ± 0 | N/A | 8.0 ± 1.7 |
| IPI00014898 | PLEC1 | PLEC isoform 1 of plectin-1 | 57.7 ± 11.9 | 9.0 ± 6.1 | 102.3 ± 13.3 |
| IPI00306543 | GDF15 | GDF15 growth/differentiation factor 15 | 4.7 ± 2.3 | 0.7 ± 1.2 | 17.3 ± 4.0 |
| IPI00019590 | PLAT | PLAT isoform 1 of tissue-type plasminogen activator | N/A | 22.3 ± 18.0 | 115.3 ± 18.7 |
| IPI00377045 | LAMA3 | LAMA3 laminin alpha-3 chain variant 1 | N/A | 6.0 ± 10.4 | 27.7 ± 2.1 |
| IPI00013890 | SFN | SFN Isoform 1 of 14-3-3 protein sigma | 0.3 ± 0.6 | 0.7 ± 0.6 | 10.3 ± 1.2 |
| IPI00297487 | CTSH | CTSH cathepsin H | N/A | 0.7 ± 0.6 | 8.3 ± 2.5 |
| IPI00029273 | MET | MET Isoform 1 of hepatocyte growth factor receptor | N/A | 13.3 ± 13.8 | 27.7 ± 1.5 |

Note: N/A (not applicable): no proteins were detected in the sample.

cells of the microenvironment. As such, proteins present in ascites may serve as potential mediators of the disease as well as provide insight into cancer progression. Levels of MUC5AC were assessed in patient ovarian cancer ascites fluid, as well as fluids from benign cyst neoplasms (Fig. 4). Overall, the protein was found to be elevated in patient

ascites fluid, compared to serous cyst fluid ($p = 0.021$), which suggests that it becomes elevated during cancer. Classification of ascites and cyst fluid into low and high levels of MUC5AC also revealed a significant difference between the two groups ($p = 0.001$, Fisher’s exact test; sensitivity = 100%; specificity = 80%; predictive accuracy = 88.9%).

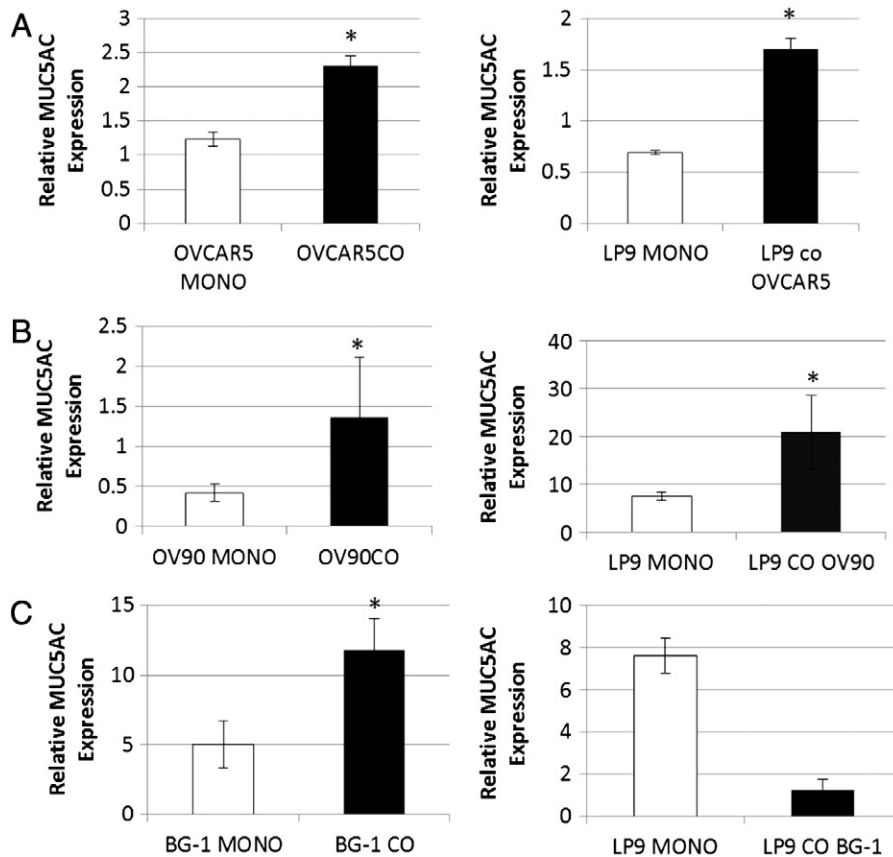


Fig. 3 – Gene expression analysis of MUC5AC in cancer and peritoneal cells grown in co-culture. Transcript levels were measured in cells grown in monocultures and co-cultures (three biological replicates) in A) LP-9/OVCAR-5 B) LP-9/BG-1, and C) LP-9/OV-90 co-cultures (*, $P \leq 0.05$, Student’s t-test). All qPCR experiments were performed in technical triplicates.

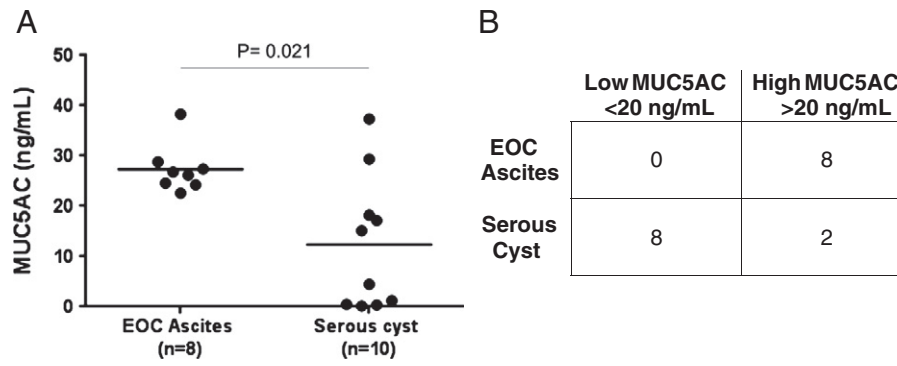


Fig. 4 – Levels of MUC5AC were measured in ovarian cancer patient ascites (n = 8) and benign ovarian serous cyst fluid (n = 10) **A**) Significant differences in MUC5AC levels (ng/mL) were observed between the two conditions (*, $P \leq 0.05$, Mann–Whitney test). **B**) 2 × 2 contingency table representing the distribution of ascites and serous cyst fluid cases with low and high levels of MUC5AC ($P = 0.001$, Fisher’s exact test; sensitivity = 100%; specificity = 80%; predictive accuracy = 88.9%). EOC, epithelial ovarian carcinoma.

4.6. Immunocytochemistry reveals elevated MUC5AC in cancer-peritoneal cell co-cultures

To confirm the upregulation of MUC5AC during cancer-peritoneal interaction, immunocytochemistry was performed, in which fixed cells were stained for the protein of interest (Fig. 5). No antibody controls were also performed to ensure that there was no background staining present (data not shown). Staining of monocultures revealed low MUC5AC expression in the LP-9 cell line and an absence of staining in the OV-90, BG-1, and OVCAR-5 monocultures. In contrast, increased intensity of staining was observed in all three co-cultures, particularly in OV-90 and OVCAR-5 co-cultures, which suggests that MUC5AC becomes elevated during ovarian cancer attachment and growth on the mesothelium.

5. Discussion

Along with other mechanisms of metastasis, such as the intravasation of cancer cells into blood and lymphatic cells and subsequent extravasation at distant sites, the formation of peritoneal implants from the adhesion of tumor cells to the mesothelium is also important for the establishment of distant metastases. Given that patients diagnosed at an advanced stage have a poor clinical outcome, an increased understanding of how tumor cells interact with peritoneum is essential for the development of therapies that prevent or target peritoneal attachment and invasion.

In this study, we sought to characterize proteomic changes that occur as a result of the interaction between cancer and

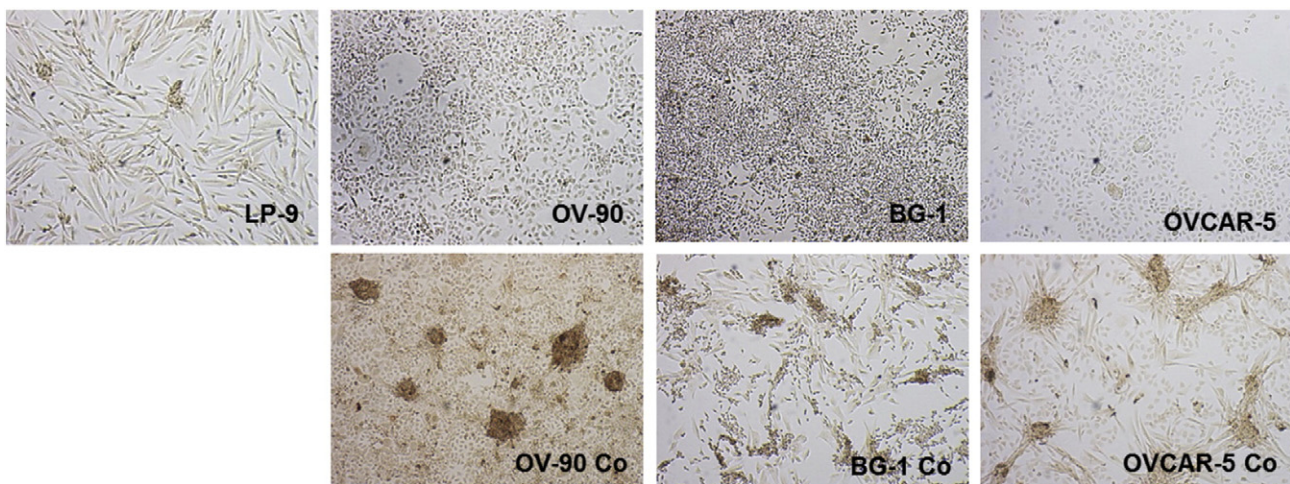


Fig. 5 – Immunocytochemistry analysis assessing MUC5AC expression in OVCAR-5 and LP-9; BG-1 and LP-9; OV-90 and LP-9 co-cultures and monocultures. MUC5AC expression was elevated in all co-cultures, while it displayed low expression in peritoneal cells, and absent in cancer monocultures. All images are displayed at ×40 magnification.

mesothelial cells. Although previous studies have also incorporated the use of mass spectrometry to identify one or two mediators of peritoneal metastasis [18], our approach is the first to provide a global snapshot of all dysregulated proteins during the crosstalk of these two cell types. Specifically, LC-MS/MS was used for the proteomic profiling of conditioned media from an *in vitro* co-culture model between ovarian cancer (OVCAR-5) and peritoneal (LP-9) cells, and their respective monoculture secretomes. Overall, our analysis resulted in the identification of 2554 non-redundant proteins in all three experimental conditions, whereby a subset of proteins were identified solely in the co-culture secretomes. After applying a set of stringent filtering criteria, we were able to narrow down our candidates using two different approaches, which were based on spectral counting and monoculture exclusion. In total, 49 proteins displayed low secretion or absence in peritoneal or cancer cells in comparison to the co-culturing of the two cell populations. In order to confirm the feasibility of our approach, we examined whether proteins that have been previously linked to the peritoneal dissemination of ovarian tumors were identified through our MS-based analysis. For example, to date, several molecules have been associated with EOC metastasis, including TGF β 1p, ITG β 1, VCAM1, MET, CD44H, ICAM-1, FN, CX(3)CL1, and mesothelin, which assist in the attachment of malignant cells to extracellular matrix (ECM) components or to mesothelial cells [9–11,14,15,18,25–27]. As such, all of these proteins were observed in the conditioned media of our co-cultures, with some displaying increased secretion. Although the identification of these molecules strengthens the validity of our approach, we should also acknowledge the limitations of our experimental system. For instance, our co-culture model represents a two-dimensional system, and therefore, does not entirely recapitulate EOC progression as it occurs *in vivo*, as it lacks the contribution of biological and cellular components belonging to the tumor microenvironment, including the underlying ECM. Moreover, given that EOC is a heterogeneous disease, the use of one cell line is not sufficient to capture the entire proteome that is representative of all ovarian cancers, and therefore, proteomic secretions may be subjected to cell line biases. However, we postulated that because cancer-peritoneal attachment is a very specific interaction, similar proteomic alterations and molecules will be recruited, regardless of the cell line used, but, how abundantly expressed they are will vary across different cell lines. Thus, we further evaluated our top candidate, MUC5AC, in two other comparable model systems using the ovarian cancer cell lines, OV-90 and BG-1. Interestingly, differences in expression were observed in mesothelial cells when they were co-cultured with BG-1 cancer cells, compared to those cultured OVCAR-5 and OV-90 cells, which suggests that different cell lines have specific effects on mesothelial cells.

After analyzing the gene expression levels of our top candidates, we observed a significant elevation of mucin 5AC in both the ovarian cancer (OVCAR-5) and mesothelial (LP-9) cell lines when they were stimulated with each other's conditioned media (indirect one-way co-cultures). Other promising candidates that were elevated including HYAL1, LRG1, and TFPI2, have all been previously linked to ovarian cancer [28–30]. In addition, increased expression of MUC5AC

was also observed in two-way indirect co-culture models using OVCAR-5, OV-90, and BG-1 cell lines, as well as in patient ascites fluid, which indicates that it may have a putative role in the pathophysiology of the disease. However, further studies are required to evaluate whether MUC5AC has a direct role in promoting ovarian cancer progression, and whether it is a driver or passenger during metastasis. Furthermore, our immunocytochemistry analysis revealed increased MUC5AC expression in the co-cultures of all cell lines; however, the bulk of its secretion appears to be derived from peritoneal cells.

Interestingly, previous immunohistochemistry and biochemical studies have revealed an elevated expression of MUC5AC in ovarian tumor samples compared to normal tissue, primarily those of the mucinous subtype [31,32]. However, little or no expression is often observed in ovarian serous carcinomas [33,34], suggesting that its induction may be mediated by the communication between cancerous cells and the mesothelium through the exchange of soluble factors during peritoneal metastasis [34]. In our study, this theory is exemplified by the lack of MUC5AC expression in cancer cells cultured alone. However, in a recent study, mucin 5AC was elevated in the interstitial fluid and tumor lysates of endometrioid, mucinous, and serous ovarian carcinomas compared to control healthy ovarian tissue, but displayed marked heterogeneity among the subgroups of patients [32].

MUC5AC belongs to the mucin family of secreted and transmembrane glycoproteins, which have multifaceted roles in various diseases and are commonly dysregulated during inflammation and cancer [35]. Thus far, few transmembrane mucins have been associated with aberrant expression in ovarian cancer, particularly, mucin 16 (or CA125), which is elevated in ovarian cancer patient sera and is clinically used as a monitoring biomarker [36]. Apart from its role in the clinic, one group has identified a binding domain for CA125 on mesothelin, a cell-surface protein expressed by both cancer and peritoneal cells [37]. This binding domain may facilitate the adhesion of both cell types, and thus, has major implications for EOC tumorigenesis [37]. Interestingly, MUC4, a transmembrane mucin that is overexpressed in ovarian tumors, which has been shown to increase the motility and invasiveness of ovarian cancer cells through the induction of epithelial-to-mesenchymal transition was also elevated in our co-cultures [38–40]. To date, few studies have evaluated the pathophysiological association of MUC5AC with respect to ovarian cancer, as aberrant expression has mainly been linked to colorectal, pancreatic, and gastric carcinomas, in addition to the regulation of airway epithelial cells [33,34]. Moreover, in these studies, its expression was often correlated with more aggressive and advanced stage cancers [33,34]. As a result, mucin 5AC has been shown to enhance the invasive properties of cancer cells undergoing metastasis [35]. In a recent study, the knockdown of MUC5AC in pancreatic cancer cells resulted in reduced adhesion, invasion, and metastasis, through the down-regulation of integrins, MMP-3 and VEGF [41]. Moreover, in *in vivo* xenograft studies, it was shown that the knockdown of MUC5AC suppressed tumor growth and tumorigenesis of pancreatic cancer, while using *in vitro* cell lines, MUC5AC was shown to inhibit TRAIL-induced apoptosis [42,43]. From the above observations, it is evident that

MUC5AC plays a major role in cancer progression, and the mechanisms by which it supports ovarian cancer metastasis should be further explored. Given that the adhesion and invasion of ovarian cancer to the peritoneum relies heavily on several integrin molecules, it would be interesting to determine whether MUC5AC also regulates their expression, similar to what occurs in pancreatic cancer.

In addition to cancer, MUC5AC is also induced in human bronchial epithelial cells by the proinflammatory cytokines, TNF- α , IL-1 β and IL-17A, through the activation of the NF- κ B pathway, which are all known pathways/mediators that contribute to metastatic EOC [44–47]. Previous groups have demonstrated that pre-incubation of mesothelial monolayers with inflammatory cytokines including TNF- α , IL-1 β , and IL-6 enhances their adhesion to colorectal cancer cells and alters their own morphology [25,48,49]. Given that TNF- α is actively produced by ovarian cancer cells, and is a potent stimulator of MUC5AC, we postulate that one mechanism by which TNF- α increases the adhesion between cancer and peritoneal cells may be mediated through the release of MUC5AC; however, whether its induction acts in a similar way in ovarian cancer has yet to be elucidated with additional experiments.

Overall, in the present study, we performed a comprehensive proteomic analysis to characterize alterations in protein secretion that occur during ovarian cancer–peritoneal interaction. Our findings provide evidence that MUC5AC becomes elevated during the direct co-culturing of cancer and mesothelial cells. As such, future efforts should aim to delineate its functional relevance in terms of cancer cell migration and invasion of the mesothelium, using appropriate in vitro and in vivo model systems, in addition to determining the underlying mechanisms that cause its induction.

Supplementary data to this article can be found online at <http://dx.doi.org/10.1016/j.jprot.2014.03.042>.

Transparency Document

The Transparency document associated with this article can be found in the online version.

Acknowledgments

The authors would like to thank Antoninus Soosaipillai and Azza Eissa for technical help. N.M. is a recipient of the Canadian Institutes of Health Research (CIHR) Frederick Banting and Charles Best Canada Graduate Scholarship.

REFERENCES

- [1] Siegel R, Naishadham D, Jemal A. Cancer statistics, 2013. *Cancer J Clin* 2013;63:11–30.
- [2] Pignata S, Cannella L, Leopardo D, Pisano C, Bruni GS, Facchini G. Chemotherapy in epithelial ovarian cancer. *Cancer Lett* 2011;303:73–83.
- [3] Vaughan S, Coward JI, Bast Jr RC, Berchuck A, Berek JS, Brenton JD, et al. Rethinking ovarian cancer: recommendations for improving outcomes. *Nat Rev Cancer* 2011;11:719–25.
- [4] Puiffe ML, Le Page C, Filali-Mouhim A, Zietarska M, Ouellet V, Tonin PN, et al. Characterization of ovarian cancer ascites on cell invasion, proliferation, spheroid formation, and gene expression in an in vitro model of epithelial ovarian cancer. *Neoplasia* 2007;9:820–9.
- [5] Meunier L, Puiffe ML, Le Page C, Filali-Mouhim A, Chevrette M, Tonin PN, et al. Effect of ovarian cancer ascites on cell migration and gene expression in an epithelial ovarian cancer in vitro model. *Transl Oncol* 2010;3:230–8.
- [6] Cai J, Tang H, Xu L, Wang X, Yang C, Ruan S, et al. Fibroblasts in omentum activated by tumor cells promote ovarian cancer growth, adhesion and invasiveness. *Carcinogenesis* 2012;33:20–9.
- [7] Musrap N, Diamandis EP. Revisiting the complexity of the ovarian cancer microenvironment—clinical implications for treatment strategies. *Mol Cancer Res* 2012;10:1254–64.
- [8] Ren J, Xiao YJ, Singh LS, Zhao X, Zhao Z, Feng L, et al. Lysophosphatidic acid is constitutively produced by human peritoneal mesothelial cells and enhances adhesion, migration, and invasion of ovarian cancer cells. *Cancer Res* 2006;66:3006–14.
- [9] Cannistra SA, Kansas GS, Niloff J, DeFranzo B, Kim Y, Ottensmeier C. Binding of ovarian cancer cells to peritoneal mesothelium in vitro is partly mediated by CD44H. *Cancer Res* 1993;53:3830–8.
- [10] Gardner MJ, Jones LM, Catterall JB, Turner GA. Expression of cell adhesion molecules on ovarian tumour cell lines and mesothelial cells, in relation to ovarian cancer metastasis. *Cancer Lett* 1995;91:229–34.
- [11] Lessan K, Aguiar DJ, Oegema T, Siebensohn L, Skubitz AP. CD44 and beta1 integrin mediate ovarian carcinoma cell adhesion to peritoneal mesothelial cells. *Am J Pathol* 1999;154:1525–37.
- [12] Niedbala MJ, Crickard K, Bernacki RJ. Interactions of human ovarian tumor cells with human mesothelial cells grown on extracellular matrix. An in vitro model system for studying tumor cell adhesion and invasion. *Exp Cell Res* 1985;160:499–513.
- [13] Rieppi M, Vergani V, Gatto C, Zanetta G, Allavena P, Taraboletti G, et al. Mesothelial cells induce the motility of human ovarian carcinoma cells. *Int J Cancer* 1999;80:303–7.
- [14] Strobel T, Cannistra SA. Beta1-integrins partly mediate binding of ovarian cancer cells to peritoneal mesothelium in vitro. *Gynecol Oncol* 1999;73:362–7.
- [15] Slack-Davis JK, Atkins KA, Harrer C, Hershey ED, Conaway M. Vascular cell adhesion molecule-1 is a regulator of ovarian cancer peritoneal metastasis. *Cancer Res* 2009;69:1469–76.
- [16] Tzuman YC, Sapoznik S, Granot D, Nevo N, Neeman M. Peritoneal adhesion and angiogenesis in ovarian carcinoma are inversely regulated by hyaluronan: the role of gonadotropins. *Neoplasia* 2010;12:51–60.
- [17] Karagiannis GS, Petraki C, Prassas I, Saraon P, Musrap N, Dimitromanolakis A, et al. Proteomic signatures of the desmoplastic invasion front reveal collagen type XII as a marker of myofibroblastic differentiation during colorectal cancer metastasis. *Oncotarget* 2012;3:267–85.
- [18] Ween MP, Lokman NA, Hoffmann P, Rodgers RJ, Ricciardelli C, Oehler MK. Transforming growth factor-beta-induced protein secreted by peritoneal cells increases the metastatic potential of ovarian cancer cells. *Int J Cancer* 2011;128:1570–84.
- [19] Tien CL, Lin CH, Lin TH, Wen FC, Su CW, Fan SS, et al. Secreted cyclophilin A induction during embryo implantation in a model of human trophoblast–endometrial epithelium interaction. *Eur J Obstet Gynecol Reprod Biol* 2012;164:55–9.
- [20] Zeng X, Yang P, Chen B, Jin X, Liu Y, Zhao X, et al. Quantitative secretome analysis reveals the interactions between epithelia and tumor cells by in vitro modulating colon cancer microenvironment. *J Proteomics* 2013;89:51–70.

- [21] Garcion C, Baltensperger R, Fournier T, Pasquier J, Schnetzer MA, Gabriel JP, et al. FiRe and microarrays: a fast answer to burning questions. *Trends Plant Sci* 2006;11:320–2.
- [22] Ahmed AA, Etemadmoghadam D, Temple J, Lynch AG, Riad M, Sharma R, et al. Driver mutations in TP53 are ubiquitous in high grade serous carcinoma of the ovary. *J Pathol* 2010;221:49–56.
- [23] Kulbe H, Thompson R, Wilson JL, Robinson S, Hagemann T, Fatah R, et al. The inflammatory cytokine tumor necrosis factor- α generates an autocrine tumor-promoting network in epithelial ovarian cancer cells. *Cancer Res* 2007;67:585–92.
- [24] Doherty JA, Rossing MA, Cushing-Haugen KL, Chen C, Van Den Berg DJ, Wu AH, et al. ESR1/SYNE1 polymorphism and invasive epithelial ovarian cancer risk: an Ovarian Cancer Association Consortium study. *Cancer Epidemiol Biomarkers Prev* 2010;19:245–50.
- [25] Ziprin P, Ridgway PF, Pfistermuller KL, Peck DH, Darzi AW. ICAM-1 mediated tumor-mesothelial cell adhesion is modulated by IL-6 and TNF- α : a potential mechanism by which surgical trauma increases peritoneal metastases. *Cell Commun Adhes* 2003;10:141–54.
- [26] Kim M, Rooper L, Xie J, Kajdacsy-Balla AA, Barbolina MV. Fractalkine receptor CX(3)CR1 is expressed in epithelial ovarian carcinoma cells and required for motility and adhesion to peritoneal mesothelial cells. *Mol Cancer Res* 2012;10:11–24.
- [27] Burleson KM, Casey RC, Skubitz KM, Pambuccian SE, Oegema Jr TR, Skubitz AP. Ovarian carcinoma ascites spheroids adhere to extracellular matrix components and mesothelial cell monolayers. *Gynecol Oncol* 2004;93:170–81.
- [28] Yoffou PH, Edjekouane L, Meunier L, Tremblay A, Provencher DM, Mes-Masson AM, et al. Subtype specific elevated expression of hyaluronidase-1 (HYAL-1) in epithelial ovarian cancer. *PLoS One* 2011;6:e20705.
- [29] Andersen JD, Boylan KL, Jemmerson R, Geller MA, Misemer B, Harrington KM, et al. Leucine-rich alpha-2-glycoprotein-1 is upregulated in sera and tumors of ovarian cancer patients. *J Ovarian Res* 2010;3:21.
- [30] Zhang Q, Hu G, Yang Q, Dong R, Xie X, Ma D, et al. A multiplex methylation specific PCR assay for the detection of early-stage ovarian cancer using cell-free serum DNA. *Gynecol Oncol* 2013;130:132–9.
- [31] Ji H, Isacson C, Seidman JD, Kurman RJ, Ronnett BM. Cytokeratins 7 and 20, Dpc4, and MUC5AC in the distinction of metastatic mucinous carcinomas in the ovary from primary ovarian mucinous tumors: Dpc4 assists in identifying metastatic pancreatic carcinomas. *Int J Gynecol Pathol* 2002;21:391–400.
- [32] Haslene-Hox H, Oveland E, Woie K, Salvesen HB, Wiig H, Tenstad O. Increased WD-repeat containing protein 1 in interstitial fluid from ovarian carcinomas shown by comparative proteomic analysis of malignant and healthy gynecological tissue. *Biochim Biophys Acta* 1834;2013:2347–59.
- [33] Lau SK, Weiss LM, Chu PG. Differential expression of MUC1, MUC2, and MUC5AC in carcinomas of various sites: an immunohistochemical study. *Am J Clin Pathol* 2004;122:61–9.
- [34] Han L, Pansare V, Al-Abbadi M, Husain M, Feng J. Combination of MUC5ac and WT-1 immunohistochemistry is useful in distinguishing pancreatic ductal carcinoma from ovarian serous carcinoma in effusion cytology. *Diagn Cytopathol* 2009;38:333–6.
- [35] Kufe DW. Mucins in cancer: function, prognosis and therapy. *Nat Rev Cancer* 2009;9:874–85.
- [36] Kobayashi E, Ueda Y, Matsuzaki S, Yokoyama T, Kimura T, Yoshino K, et al. Biomarkers for screening, diagnosis, and monitoring of ovarian cancer. *Cancer Epidemiol Biomarkers Prev* 2012;21:1902–12.
- [37] Kaneko O, Gong L, Zhang J, Hansen JK, Hassan R, Lee B, et al. A binding domain on mesothelin for CA125/MUC16. *J Biol Chem* 2009;284:3739–49.
- [38] Chauhan SC, Singh AP, Ruiz F, Johansson SL, Jain M, Smith LM, et al. Aberrant expression of MUC4 in ovarian carcinoma: diagnostic significance alone and in combination with MUC1 and MUC16 (CA125). *Mod Pathol* 2006;19:1386–94.
- [39] Ponnusamy MP, Singh AP, Jain M, Chakraborty S, Moniaux N, Batra SK. MUC4 activates HER2 signalling and enhances the motility of human ovarian cancer cells. *Br J Cancer* 2008;99:520–6.
- [40] Ponnusamy MP, Lakshmanan I, Jain M, Das S, Chakraborty S, Dey P, et al. MUC4 mucin-induced epithelial to mesenchymal transition: a novel mechanism for metastasis of human ovarian cancer cells. *Oncogene* 2010;29:5741–54.
- [41] Yamazoe S, Tanaka H, Sawada T, Amano R, Yamada N, Ohira M, et al. RNA interference suppression of mucin 5AC (MUC5AC) reduces the adhesive and invasive capacity of human pancreatic cancer cells. *J Exp Clin Cancer Res* 2010;29:53.
- [42] Hoshi H, Sawada T, Uchida M, Saito H, Iijima H, Toda-Agetsuma M, et al. Tumor-associated MUC5AC stimulates in vivo tumorigenicity of human pancreatic cancer. *Int J Oncol* 2011;38:619–27.
- [43] Hoshi H, Sawada T, Uchida M, Iijima H, Kimura K, Hirakawa K, et al. MUC5AC protects pancreatic cancer cells from TRAIL-induced death pathways. *Int J Oncol* 2013;42:887–93.
- [44] Fujisawa T, Velichko S, Thai P, Hung LY, Huang F, Wu R. Regulation of airway MUC5AC expression by IL-1 β and IL-17A; the NF- κ B paradigm. *J Immunol* 2009;183:6236–43.
- [45] Song KS, Lee WJ, Chung KC, Koo JS, Yang EJ, Choi JY, et al. Interleukin-1 β and tumor necrosis factor- α induce MUC5AC overexpression through a mechanism involving ERK/p38 mitogen-activated protein kinases-MSK1-CREB activation in human airway epithelial cells. *J Biol Chem* 2003;278:23243–50.
- [46] Mochizuki Y, Nakanishi H, Kodera Y, Ito S, Yamamura Y, Kato T, et al. TNF- α promotes progression of peritoneal metastasis as demonstrated using a green fluorescence protein (GFP)-tagged human gastric cancer cell line. *Clin Exp Metastasis* 2004;21:39–47.
- [47] Hernandez L, Hsu SC, Davidson B, Birrer MJ, Kohn EC, Annunziata CM. Activation of NF- κ B signaling by inhibitor of NF- κ B kinase beta increases aggressiveness of ovarian cancer. *Cancer Res* 2010;70:4005–14.
- [48] van Grevenstein WM, Hofland LJ, van Rossen ME, van Koetsveld PM, Jeekel J, van Eijck CH. Inflammatory cytokines stimulate the adhesion of colon carcinoma cells to mesothelial monolayers. *Dig Dis Sci* 2007;52:2775–83.
- [49] Stadlmann S, Raffener R, Amberger A, Margreiter R, Zeimet AG, Abendstein B, et al. Disruption of the integrity of human peritoneal mesothelium by interleukin-1 β and tumor necrosis factor- α . *Virchows Arch* 2003;443:678–85.